

STOCHASTIC BUCKLING ANALYSES OF LAMINATED COMPOSITE PLATES UNDER HYGROTHERMAL, GEOMETRIC AND MATERIAL UNCERTAINTIES MODELED AS NON-GAUSSIAN RANDOM FIELDS

Henrique E. A. A. dos Santos^{1,2} & Domingos A. Rade²

¹Embraer S.A., Avenida Brigadeiro Faria Lima, 2170, São José dos Campos, São Paulo, Brazil, 12227-901
 ²Aeronautics Institute of Technology, Praça Mal. Eduardo Gomes 50, Vila das Acácias, São José dos Campos, São Paulo, Brazil, 12228-900

Abstract

Abstract. The combined effects of hygrothermal conditions and material characteristics on the buckling response of laminated composite plates are numerically studied in this paper. As the physical mechanisms determining the environmental and operational conditions are very complex, the temperature and moisture variations throughout a structure can hardly be controlled in many cases of industrial interest. Also, inherent material variability are present in the structure domain due to manufacturing processes, specially involving composite materials. As a consequence, the characterization of the environmental and material influences as random quantities is more appropriate. Motivated by situations found in aerospace structural engineering, this paper aims to investigate the influence of space-dependent random hygrothermal conditions, geometry and material properties on the critical buckling loads of composite laminate plates. The main contributions lie in the consideration of simultaneous random quantities affecting the structural stability and combined influences of the environmental effects both on the degradation of material properties and the occurrence of stresses induced by hygrothermal changes. Under the hypotheses of the Classical Lamination Theory, a finite element model is employed to perform buckling analysis considering hygrothermal and mechanical loadings, where the degradation of material properties is predicted using a micromechanical approach. The space-dependent fluctuations of temperature, fiber-direction angle, ply thickness, and fiber volume fraction are discretized as stationary two-dimensional random fields by the Karhunen-Loève expansion (KLE), considering non-Gaussian marginal distribution functions, where the simulation are conducted using a methodology based on the Iterative Translation Approximation Method (ITAM). Monte Carlo Simulation, combined with the Latin Hypercube Sampling, is used to generate sampling-based statistics for the critical buckling load considering different values of standard deviations and correlation lengths associated to the random fields. From the simulation scenarios analyzed, the necessity of accounting for random environmental and material uncertainties in the analysis and design of reliable and robust composite structures is highlighted.

Keywords: uncertainty quantification, hygrothermal loads, buckling, non-Gaussian random field, micromechanical modeling, laminated composite plates.

1. INTRODUCTION

Although composite materials have increasingly been used in the aerospace industry due to their superior properties, such as high strength-to-weight ratios, high impact and corrosion resistance, and larger design space, some inconveniences regarding the exposition to changes in environmental conditions arise. In particular, in aerospace applications, severe temperature and moisture variations are common and, consequently, composite materials experience significant effects on their structural responses [1]. In addition, as stated in [2], significant variability in material properties of composites are often present, as composite laminates are manufactured by complex processes, which may induce voids and variations in volume fractions of fibers and matrix, imperfections in bonding between

components, damage and misalignment in fibers, residual stresses, non-uniform curing process, among others. Those uncertainties increase the variability in the overall stiffness and strength of the material.

The environmental conditions can degrade the composite material properties through physical mechanisms of heat conduction and moisture diffusion. According to [1], increase in temperature causes softening of the polymer matrix, which can be aggravated when the glass transition region (transition from glassy to rubbery behavior) is brought to lower temperatures as a result of moisture increase. In addition, the temperature and/or moisture increase leads to expansion/swelling of the polymer matrix and, as fibers are practically insensitive to hygrothermal changes, residual stresses develop, leading to modifications of stress and strain distributions over the structure.

The degradation in lamina material properties at elevated temperature and moisture is analyzed in [3] regarding the deflection, buckling and natural frequency of thick composite laminates. In [4], a micromechanics model was used to predict the elastic and hygrothermal properties of the fiber reinforced composite material considered to be dependent on temperature and moisture concentration. Considerable deterioration in the flexural response of the laminated composite plate was obtained. The influence of temperature-dependent material properties was also investigated in [5], where the thermomechanical buckling behavior of variable angle tow (VAT) laminates is analyzed.

The previously cited studies consider purely deterministic approaches in the analyses involving material properties of composites and induced stresses under hygrothermal conditions, which, in many cases of practical interest, may show to be inadequate. Within stochastic frameworks, hygrothermal buckling loads of straight-fiber laminated plates subjected to uniform temperature/moisture changes were analyzed in [6], considering random variations of lamina thickness and material properties. In [7], the influence of uncertainties related to lamina properties, fiber orientations and thermal expansion coefficients on the thermal buckling response of variable stiffness composite laminate is studied for different boundary conditions and lamination sequences. Regarding the hygrothermal buckling response of laminated composite plates, reference [8] considers random thermoelastic properties, both independent and dependent of temperature.

For the stochastic characterization of uncertain variables, some quantities are more appropriately modeled as space-distributed random uncertainties. The complexity involving physical mechanisms of heat and moisture transfer makes the temperature and moisture variations at different points of a structure hard to be predicted and controlled and, as a consequence, these environmental changes can be more appropriately characterized as spatially varying random quantities. Analogously, the variations in material characteristics of a composite laminate due to the manufacturing processes, besides the intrinsically fluctuations in properties of its inner constituents, seem also to be more adequately modeled as stochastic space-dependent.

The stochastic characterization of space-dependent quantities encompasses the concept of random field, which, for convenient numerical manipulation, is dealt with by using discretization techniques, such as the Karhunen-Loève Expansion (KLE) [9]. The KLE was originally used for simulating Gaussian stochastic processes and, for this reason, the vast majority of KLE applications are devoted to the discretization of this category of random fields [10]. However, non-Gaussian random fields can be found in many situations of practical interest, which requires especial techniques for the application of KLE. Among many other investigations, in [11], non-stationary and strongly non-Gaussian stochastic processes are simulated using an efficient methodology based on the Iterative Translation Approximation Method (ITAM) and the KLE, denoted by KL-ITAM, which is used in the present work. Spatially varying variables discretized by KLE have been considered in some studies of composite laminates. In [12], the effect of spatial randomness of micro- and macro-mechanical material properties is quantified to characterize the probabilistic descriptions of stochastic dynamics and stability of composite laminates based on KLE. The lamina fiber volume, and consequently the material properties through the mixture rule, is represented by a two-dimensional random field discretized by KLE in [13], where the polynomial chaos expansion (PCE) was used to predict aeroelastic responses. Reference [14] also considered spatially varying fiber volume content, together with fiber misalignment random fields, to be discretized by KLE to stochastically characterize the buckling response of variable stiffness composites.

Regarding the space-distributed stochastic characterization of environmental conditions, [15] analyzed the stochastic thermal buckling of composite plates using KLE to discretize the temperature distribution, which also leads to spatially varying mechanical properties, as temperature-dependent properties were considered.

In the context delineated above, the present paper proposes the stochastic evaluation of the buckling response of laminated composite plates accounting for uncertainties affecting the hygrothermal conditions and material characteristics. Fluctuations on temperature, fiber-direction angle, ply thickness, and fiber volume fraction throughout a composite plate are discretizatized by KLE as stationary, non-Gaussian, two-dimensional random fields. As a consequence, using the micromechanical approach, randomness in environmental-dependent material properties and in hygrothermally-induced stresses are simultaneously included in the plate modeling under the hypotheses of the classical lamination theory (CLT). Moisture content is also considered to vary spatially over the structure due to fiber volume variations. Then, for different standard deviations and correlation lengths assigned to the random fields, the uncertainty quantification of the critical buckling load is conducted through stochastic numerical analyses performed by Monte Carlo Simulation (MCS) combined with the Latin Hypercube Sampling (LHS).

2. FORMULATION

2.1 Random fields discretized by KLE

For a rectangular plate with dimensions a and b in directions x and y, respectively, as illustrated in Figure 1, a continuous two-dimensional random field $W(\zeta, \eta, \Theta)$ can be described using a truncated KLE in terms of the normalized coordinates $\zeta = 2x/a$ and $\eta = 2y/b$, as follows [9]:

$$W(\zeta, \eta, \Theta) = \bar{W}(\zeta, \eta) + \Delta W(\zeta, \eta, \Theta) = \bar{W}(\zeta, \eta) + \sum_{n=1}^{M} \sqrt{\lambda_n} \xi_n(\Theta) f_n(\zeta, \eta) , \qquad (1)$$

where $\bar{W}(\zeta,\eta)$ is the mean field and $\xi_n(\Theta)$ is a set of M zero-mean, unit-variance Gaussian uncorrelated random variables defined in an appropriate random space, in which Θ denotes an appropriate sample space. In addition, λ_n and $f_n(\zeta,\eta)$ are solutions (eigenvalues and eigenfunctions, respectively) of the following integral eigenvalue problem associated with an adopted covariance function $C(\zeta_1,\zeta_2;\eta_1,\eta_2)$:

$$\int_{-1}^{1} \int_{-1}^{1} C(\zeta_1, \zeta_2; \eta_1, \eta_2) f_n(\zeta_2, \eta_2) d\zeta_2 d\eta_2 = \lambda_n f_n(\zeta_1, \eta_1) , \quad n = 1, ..., M .$$
 (2)

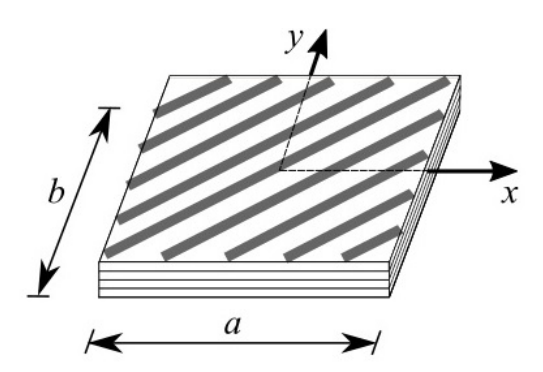


Figure 1 – Rectangular laminated composite plate.

2.1.1 Non-Gaussian random fields using KL-ITAM

As the stochastic fields considered in the present work follow non-Gaussian distributions, the methodology KL-ITAM, based on the ITAM and KLE, is used in the simulations. The methodology aims at identifying a Gaussian random field $W_G(\zeta,\eta,\Theta)$ with its respective underlying Gaussian autocorrelation function (ACF) that, when mapped using translation process theory, matches the prescribed non-Gaussian distribution and the target ACF [11].

The following steps summarize the method:

1) **Initialization of the underlying Gaussian ACF**. As the Gaussian random field to be translated has zero mean and unit variance, the following relation is used for its autocorrelation function, $R_G(\zeta_1, \zeta_2; \eta_1, \eta_2)$, to initiate the iterative process:

$$R_G(\zeta_1, \zeta_2; \eta_1, \eta_2) = \frac{1}{\sigma_N^2} C(\zeta_1, \zeta_2; \eta_1, \eta_2) , \qquad (3)$$

where σ_N and $C(\zeta_1, \zeta_2; \eta_1, \eta_2)$ are the standard deviation and the covariance function associated with the non-Gaussian random field, respectively.

2) Computation of the non-Gaussian ACF using the translation process. The normalized Gaussian correlation function is computed:

$$\rho_G(\zeta_1, \zeta_2; \eta_1, \eta_2) = \frac{R_G(\zeta_1, \zeta_2; \eta_1, \eta_2)}{\sqrt{R_G(\zeta_1, \zeta_1; \eta_1, \eta_1) R_G(\zeta_2, \zeta_2; \eta_2, \eta_2)}} . \tag{4}$$

Then, the translation process is performed:

$$R_{N}(\zeta_{1}, \zeta_{2}; \eta_{1}, \eta_{2}) = \int_{-\infty}^{\infty} \int_{-\infty}^{\infty} F_{N}^{-1} \{\Phi[w_{1}], \zeta_{1}, \eta_{1}\} F_{N}^{-1} \{\Phi[w_{2}], \zeta_{2}, \eta_{2}\} \phi\{w_{1}, w_{2}; \rho_{G}(\zeta_{1}, \zeta_{2}; \eta_{1}, \eta_{2})\} dw_{1} dw_{2},$$

$$(5)$$

where $w_1=W_G(\zeta_1,\eta_1)$, $w_2=W_G(\zeta_2,\eta_2)$, $F_N^{-1}\{\cdot,\zeta_i,\eta_i\}$ is the inverse marginal non-Gaussian cumulative distribution function (CDF) at point (ζ_i,η_i) , and Φ is the standard Gaussian CDF (i.e., zero mean and unit variance). The joint Gaussian probability density function is given as:

$$\phi\{w_1, w_2; \rho_G(\zeta_1, \zeta_2; \eta_1, \eta_2)\} = \frac{1}{2\pi\sqrt{1 - \rho_G(\zeta_1, \zeta_2; \eta_1, \eta_2)^2}} exp\left(-\frac{w_1^2 + w_2^2 - 2\rho_G(\zeta_1, \zeta_2; \eta_1, \eta_2)w_1w_2}{2(1 - \rho_G(\zeta_1, \zeta_2; \eta_1, \eta_2)^2)}\right).$$
(6)

3) **Check of convergence**. The relative difference between the estimated and the target non-Gaussian ACF can be obtained according to below:

$$err(i) = 100\sqrt{\frac{\sum_{n=0}^{N_d-1} \sum_{m=0}^{N_d-1} \left[R_N^{(i)}(\zeta_n, \zeta_m; \eta_n, \eta_m) - R_N^T(\zeta_n, \zeta_m; \eta_n, \eta_m) \right]^2}{\sum_{n=0}^{N_d-1} \sum_{m=0}^{N_d-1} \left[R_N^T(\zeta_n, \zeta_m; \eta_n, \eta_m) \right]^2}},$$
(7)

where N_d is the number of points in the discretized domain. Considering $\mu_N(\zeta_1, \eta_1)$ and $\mu_N(\zeta_2, \eta_2)$ as the means of the random field at (ζ_1, η_1) and (ζ_2, η_2) , respectively, the target non-Gaussian ACF is determined as:

$$R_N^T(\zeta_1, \zeta_2; \eta_1, \eta_2) = \mu_N(\zeta_1, \eta_1) \ \mu_N(\zeta_2, \eta_2) + C(\zeta_1, \zeta_2; \eta_1, \eta_2) \ . \tag{8}$$

The iterative process is stopped when the relative difference value is lower than a determined tolerance or when it stabilizes. In case the convergence is achieved, the process jumps to step 5, otherwise the next step (4) is performed, followed by repetition of steps 2 and 3.

4) **Update of the underlying Gaussian ACF**. While convergence is not achieved at iteration *i*, the following equation is used to update the underlying Gaussian ACF:

$$R_G^{(i+1)}(\zeta_1, \zeta_2; \eta_1, \eta_2) = \frac{R_N^T(\zeta_1, \zeta_2; \eta_1, \eta_2)}{R_N^{(i)}(\zeta_1, \zeta_2; \eta_1, \eta_2)} R_G^{(i)}(\zeta_2, \zeta_2; \eta_2, \eta_2) . \tag{9}$$

The updated ACF needs to be positive semi-definite (PSD) to be admissible. The nearest PSD ACF is then found to maintain such property. In this work, the *nearcorr* function available in Matlab is used.

5) **Simulation of the random field using KLE**. KLE is performed according described in Section 2.1 using the Gaussian ACF engendered by the iterative process to discretize a Gaussian random field. The eigenproblem given by Eq. 2 is solved numerically using the Nyström method, described in details in [16].

The generated Gaussian random field is then mapped to the non-Gaussian one using the following equation:

$$W_N(\zeta, \eta) = F_N^{-1} \{ \Phi[W_G(\zeta, \eta)], \zeta, \eta \} . \tag{10}$$

2.2 Micromechanical modeling of hygrothermal and material properties

In this work, temperature, fiber-direction angle, ply thickness, and fiber volume fraction are modeled as non-Gaussian random fields discretized by KLE, being denoted by $T(\zeta,\eta,\Theta)$, $\theta(\zeta,\eta,\Theta)$, $t(\zeta,\eta,\Theta)$ and $V_f(\zeta,\eta,\Theta)$, respectively. The stochastic elastic and hygrothermal properties of a single lamina, taking into account the dependence of environmental conditions, are predicted using the micromechanical approach.

In accordance with the fact that polymeric matrices are predominantly affected by changes in hygrothermal conditions, the following empirical matrix mechanical and hygrothermal property retention ratios, respectively, duly adapted to consider random space-dependent temperature field $T(\zeta, \eta, \Theta)$, are used to estimate degradation of the material properties [17, 18]:

$$F_m(\zeta, \eta, \Theta) = \frac{P}{P_o} = \left[\frac{T_{gw} - T(\zeta, \eta, \Theta)}{T_{go} - T_o} \right]^{0.5} \quad , \quad F_h(\zeta, \eta, \Theta) = \frac{1}{F_m(\zeta, \eta, \Theta)} \quad , \tag{11}$$

where P refers to the matrix strength or stiffness after hygrothermal degradation and P_o is the reference matrix strength or stiffness before degradation. In addition, considering all temperatures in ${}^{\circ}F$, T_o denotes the test temperature at which P_o is measured, and T_{go} and T_{gw} are, respectively, the glass transition temperatures for reference dry and wet conditions, corresponding to property P.

The relation between T_{gw} and the absorbed moisture can be experimentally obtained and, according to [18], the following empirical relation is suggested:

$$T_{gw}(\zeta, \eta, \Theta) = (0.005M_r^2 - 0.10M_r + 1.0) T_{go}$$
, (12)

where M_r denotes the weight percent of moisture in the matrix.

Based on [1], the stochastic tensile moduli along and perpendicular to the fiber direction, shear modulus, longitudinal and transverse coefficients of thermal and hygroscopic expansion for an individual lamina, neglecting the presence of voids, can be written, respectively, as follows:

$$E_1(\zeta, \eta, \Theta) = E_{f1}V_f(\zeta, \eta, \Theta) + F_m(\zeta, \eta, \Theta)E_mV_m, \qquad (13)$$

$$E_{2}(\zeta, \eta, \Theta) = F_{m}(\zeta, \eta, \Theta) E_{m} \left[1 - \sqrt{V_{f}(\zeta, \eta, \Theta)} + \frac{\sqrt{V_{f}(\zeta, \eta, \Theta)}}{1 - \sqrt{V_{f}(\zeta, \eta, \Theta)} \left(1 - \frac{F_{m}(\zeta, \eta, \Theta)E_{m}}{E_{f2}} \right)} \right], \quad (14)$$

$$G_{12}(\zeta, \eta, \Theta) = F_m(\zeta, \eta, \Theta)G_m \left[1 - \sqrt{V_f(\zeta, \eta, \Theta)} + \frac{\sqrt{V_f(\zeta, \eta, \Theta)}}{1 - \sqrt{V_f(\zeta, \eta, \Theta)} \left(1 - \frac{F_m(\zeta, \eta, \Theta)G_m}{G_{f12}}\right)} \right], \quad (15)$$

$$\alpha_{1}(\zeta, \eta, \Theta) = \frac{E_{f}\alpha_{f}V_{f}(\zeta, \eta, \Theta) + F_{m}(\zeta, \eta, \Theta)E_{m}F_{h}(\zeta, \eta, \Theta)\alpha_{m}V_{m}}{E_{f}V_{f}(\zeta, \eta, \Theta) + F_{m}(\zeta, \eta, \Theta)E_{m}V_{m}},$$
(16)

$$\beta_1(\zeta, \eta, \Theta) = \frac{E_f \beta_f V_f(\zeta, \eta, \Theta) + F_m(\zeta, \eta, \Theta) E_m F_h(\zeta, \eta, \Theta) \beta_m V_m}{E_f V_f(\zeta, \eta, \Theta) + F_m(\zeta, \eta, \Theta) E_m V_m},$$
(17)

$$\alpha_2(\zeta, \eta, \Theta) = (1 + \nu_m) F_h(\zeta, \eta, \Theta) \alpha_m V_m + (1 + \nu_f) \alpha_f V_f(\zeta, \eta, \Theta) - \alpha_1 \nu_{12} , \qquad (18)$$

$$\beta_2(\zeta, \eta, \Theta) = (1 + \nu_m) F_h(\zeta, \eta, \Theta) \beta_m V_m + (1 + \nu_f) \beta_f V_f(\zeta, \eta, \Theta) - \beta_1 \nu_{12} , \qquad (19)$$

where the subscripts f and m refer to fiber and matrix, respectively, and subscripts 1 and 2 denote the quantities along the longitudinal and transverse directions of the fibers, respectively.

The sum of volume fractions of fiber and matrix (V_m) equals 1 and the Poisson's ratio v_{12} is considered not to be hygrothermally degraded.

Also, as a consequence of space-dependent fiber volume, the moisture content in the composite material is considered to be stochastically space-distributed. Although moisture absorption varies with time when the material is exposed to ambient conditions, one assumes the condition of fully saturated equilibrium with the maximum absorbed moisture. Based on [19] and using the rule of mixture, the stochastic moisture content in the composite (M_c) can be estimated as follows:

$$M_c(\zeta, \eta, \Theta) = M_r \left(\frac{V_m \rho_m}{V_m \rho_m + V_f(\zeta, \eta, \Theta) \rho_f} \right), \tag{20}$$

where ρ_f and ρ_m are the fiber and matrix density, respectively.

2.3 Stochastic structural model

Under the stochastic fields described in previous sections and based on the assumptions of the classical lamination theory (CLT), the constitutive stress—strain relations for the *k*-th lamina of a rectangular composite laminate can be written as [20]:

$$\sigma_{k}(\zeta, \eta, \Theta) = \begin{cases} \sigma_{x}(\zeta, \eta, \Theta) \\ \sigma_{y}(\zeta, \eta, \Theta) \\ \tau_{xy}(\zeta, \eta, \Theta) \end{cases}_{k} = \bar{Q}_{k}(\zeta, \eta, \Theta) \left[\varepsilon^{0} + z_{k}(\zeta, \eta, \Theta) \kappa - \varepsilon^{H}(\zeta, \eta, \Theta) \right] , \tag{21}$$

where $\bar{Q}_k(\zeta,\eta,\Theta)$ is the stochastic transformed stiffness matrix and $z_k(\zeta,\eta,\Theta)$ is the distance from lamina's neutral surface in the thickness direction, which is stochastic as all ply thicknesses are random. In addition, the vectors of mid-plane strains, curvatures and hygrothermal strains are denoted by ε^0 , κ , and $\varepsilon^H(\zeta,\eta,\Theta)$, respectively.

The stochastic matrix $\bar{Q}_k(\zeta, \eta, \Theta)$ of the *k*-th lamina reads:

$$\bar{Q}_{k}(\zeta, \eta, \Theta) = T_{\sigma}^{-1}(\zeta, \eta, \Theta) \begin{bmatrix}
\frac{E_{1}(\zeta, \eta, \Theta)}{1 - v_{12}v_{21}} & \frac{v_{12}E_{2}(\zeta, \eta, \Theta)}{1 - v_{12}v_{21}} & 0 \\
\frac{v_{12}E_{2}(\zeta, \eta, \Theta)}{1 - v_{12}v_{21}} & \frac{E_{2}(\zeta, \eta, \Theta)}{1 - v_{12}v_{21}} & 0 \\
0 & 0 & G_{12}(\zeta, \eta, \Theta)
\end{bmatrix} T_{\sigma}^{-\top}(\zeta, \eta, \Theta) ,$$
(22)

where

$$T_{\sigma}(\zeta,\eta,\Theta) = \begin{bmatrix} \cos^2\theta(\zeta,\eta,\Theta) & \sin^2\theta(\zeta,\eta,\Theta) & 2\sin\theta(\zeta,\eta,\Theta)\cos\theta(\zeta,\eta,\Theta) \\ \sin^2\theta(\zeta,\eta,\Theta) & \cos^2\theta(\zeta,\eta,\Theta) & -2\sin\theta(\zeta,\eta,\Theta)\cos\theta(\zeta,\eta,\Theta) \\ -\sin\theta(\zeta,\eta,\Theta)\cos\theta(\zeta,\eta,\Theta) & \sin\theta(\zeta,\eta,\Theta)\cos\theta(\zeta,\eta,\Theta) & \cos^2\theta(\zeta,\eta,\Theta) - \sin^2\theta(\zeta,\eta,\Theta) \end{bmatrix}.$$

Considering T_o and M_o as the temperature and moisture content related to measured properties P_o , respectively, u, v, and w as the displacements along the direction x, y, and z, respectively, and ψ_x and ψ_y as the rotations of cross sections about the y-axis and x-axis, respectively, the strain vectors expressed in Eq. 21 are defined as follows:

$$\varepsilon^{0} = \begin{cases}
\varepsilon_{x}^{0} \\
\varepsilon_{y}^{0} \\
\gamma_{xy}^{0}
\end{cases} = \begin{bmatrix}
\partial/\partial_{x} & 0 & 0 \\
0 & \partial/\partial_{y} & 0 \\
\partial/\partial_{y} & \partial/\partial_{x} & 0
\end{bmatrix} \begin{cases}
u \\ v \\ w
\end{cases}, \quad \kappa = \begin{cases}
\kappa_{x} \\ \kappa_{y} \\ \kappa_{xy}
\end{cases} = \begin{bmatrix}
\partial/\partial_{x} & 0 \\
0 & \partial/\partial_{y} \\
\partial/\partial_{y} & \partial/\partial_{x}
\end{bmatrix} \begin{cases}
\psi_{x} \\ \psi_{y}
\end{cases},$$

$$\varepsilon^{H}(\zeta, \eta, \Theta) = T_{\varepsilon}(\zeta, \eta, \Theta) \begin{cases}
\alpha_{1}(\zeta, \eta, \Theta)[T(\zeta, \eta, \Theta) - T_{o}] + \beta_{1}(\zeta, \eta, \Theta)[M_{c}(\zeta, \eta, \Theta) - M_{o}] \\
\alpha_{2}(\zeta, \eta, \Theta)[T(\zeta, \eta, \Theta) - T_{o}] + \beta_{2}(\zeta, \eta, \Theta)[M_{c}(\zeta, \eta, \Theta) - M_{o}] \\
\alpha_{12}(\zeta, \eta, \Theta)[T(\zeta, \eta, \Theta) - T_{o}] + \beta_{12}(\zeta, \eta, \Theta)[M_{c}(\zeta, \eta, \Theta) - M_{o}]
\end{cases},$$
(23)

where

Stochastic buckling analyses of laminated composite plates under non-Gaussian random fields

$$T_{\mathcal{E}}(\zeta,\eta,\Theta) = \begin{bmatrix} \cos^2\theta(\zeta,\eta,\Theta) & \sin^2\theta(\zeta,\eta,\Theta) & -\sin\theta(\zeta,\eta,\Theta)\cos\theta(\zeta,\eta,\Theta) \\ \sin^2\theta(\zeta,\eta,\Theta) & \cos^2\theta(\zeta,\eta,\Theta) & +\sin\theta(\zeta,\eta,\Theta)\cos\theta(\zeta,\eta,\Theta) \\ 2\sin\theta(\zeta,\eta,\Theta)\cos\theta(\zeta,\eta,\Theta) & -2\sin\theta(\zeta,\eta,\Theta)\cos\theta(\zeta,\eta,\Theta) & \cos^2\theta(\zeta,\eta,\Theta) -\sin^2\theta(\zeta,\eta,\Theta) \end{bmatrix}.$$

The resultant forces (N_x, N_y, N_{xy}) and moments (M_x, M_y, M_{xy}) in a laminate plate of N laminas are then given as:

$$\begin{cases}
N_{x}(\zeta,\eta,\Theta) \\
N_{y}(\zeta,\eta,\Theta) \\
N_{xy}(\zeta,\eta,\Theta) \\
---- \\
M_{x}(\zeta,\eta,\Theta)
\end{cases} = \begin{bmatrix}
A(\zeta,\eta,\Theta) & B(\zeta,\eta,\Theta) \\
B(\zeta,\eta,\Theta) & C(\zeta,\eta,\Theta) \\
M_{y}(\zeta,\eta,\Theta) & C(\zeta,\eta,\Theta) \\
M_{xy}(\zeta,\eta,\Theta) & C(\zeta,\eta,\Theta)
\end{cases} = \begin{bmatrix}
A(\zeta,\eta,\Theta) & B(\zeta,\eta,\Theta) \\
C(\zeta,\eta,\Theta) & C(\zeta,\eta,\Theta) \\
B(\zeta,\eta,\Theta) & C(\zeta,\eta,\Theta)
\end{bmatrix} \begin{bmatrix}
\mathcal{E}_{x}^{0} \\
\mathcal{E}_{y}^{0} \\
\mathcal{E}_{y}^{0} \\
\mathcal{E}_{y}^{0} \\
\mathcal{E}_{xy}^{0}
\end{bmatrix} - \begin{bmatrix}
N_{x}^{H}(\zeta,\eta,\Theta) \\
N_{y}^{H}(\zeta,\eta,\Theta) \\
N_{xy}^{H}(\zeta,\eta,\Theta) \\
N_{xy}^{H}(\zeta,\eta,\Theta) \\
M_{y}^{H}(\zeta,\eta,\Theta) \\
M_{xy}^{H}(\zeta,\eta,\Theta)
\end{bmatrix}, (24)$$

where $A(\zeta, \eta, \Theta)$, $B(\zeta, \eta, \Theta)$, and $D(\zeta, \eta, \Theta)$ are the stochastic extensional, bending-extensional coupling, and bending stiffness matrices, respectively, written as:

$$(A(\zeta,\eta,\Theta),B(\zeta,\eta,\Theta),D(\zeta,\eta,\Theta)) = \sum_{k=1}^{N} \bar{\mathcal{Q}}_{k}(\zeta,\eta,\Theta) \int_{z_{k-1}(\zeta,\eta,\Theta)}^{z_{k}(\zeta,\eta,\Theta)} (1,z,z^{2}) dz . \tag{25}$$

The hygrothermal forces, denoted by N_x^H , N_y^H , and N_{xy}^H , and hygrothermal moments, represented by M_x^H , M_y^H , and M_{xy}^H , which are shown in Eq. 24, are expressed as:

$$\left(\begin{cases} N_x^H(\zeta, \eta, \Theta) \\ N_y^H(\zeta, \eta, \Theta) \\ N_{xy}^H(\zeta, \eta, \Theta) \end{cases}, \begin{cases} M_x^H(\zeta, \eta, \Theta) \\ M_y^H(\zeta, \eta, \Theta) \\ M_{xy}^H(\zeta, \eta, \Theta) \end{cases} \right) = \sum_{k=1}^N \bar{Q}_k(\zeta, \eta, \Theta) \varepsilon^H(\zeta, \eta, \Theta) \int_{z_{k-1}(\zeta, \eta, \Theta)}^{z_k(\zeta, \eta, \Theta)} (1, z) dz. \tag{26}$$

Based on the formulation summarized above, the stochastic equilibrium equations are obtained by finite element discretization, which leads to the following stochastic eigenvalue problem to be solved for linear buckling analysis:

$$\left[K(\Theta) - N_r^M K_G - K_H(\Theta)\right] d = 0 , \qquad (27)$$

where d is the vector of nodal displacements and rotations, N_x^M is the eigenvalue representing the buckling loads, and the structural, geometric, and hygrothermal stiffness matrices are denoted as K, K_G , and K_H , respectively. The derivation of such matrices is omitted here for the sake of concision. The finite element (FE) model is built using the commercial software MSC NASTRAN to solve the linear buckling problem and predict the buckling loads (Solution 105). CQUAD8 quadrilateral elements with eight nodes are used. Further details can be found in [21].

It is worth mentioning that a special procedure has been used to assign the values of the stochastic, space-dependent properties to each element of the mesh, according to the respective random fields.

3. NUMERICAL APPLICATIONS

3.1 Model description

For the numerical applications that follow, a square unidirectional composite laminate plate of sides 285mm, simply supported along all its edges, has been adopted. The laminate consists of 30 laminae, each of which exhibiting thickness, fiber volume fraction, and fiber-direction angle described as independent non-Gaussian two-dimensional random fields discretized by KLE, as per Eq. 1, with mean values of \bar{t} =0.20mm, \bar{V}_f =60%, and $\bar{\theta}$ according the lamination sequence [45/-45/90/45/45/90/45/90/0]_S.

The fiber and matrix properties used in the analyses are given in Table 1, together with deterministic values of elastic and hygrothermal properties of each constituent, where such values are considered to be measured at $T_o = 75^{\circ}$ F and $M_o = 0\%$, the initial environmental condition.

Also assumed to be described by KLE, according Eq. 1, the random temperature distribution over the plate is considered as a non-Gaussian two-dimensional random field with mean value of $\bar{T}=120^{\circ}\text{F}$. Such temperature random field is assumed to not vary in the out-of-plane plate. Regarding the moisture content, which is a random field due to the spatially varying fiber volume, as per Eq. 20, the weight percent of moisture in the epoxy matrix under fully saturated equilibrium is assumed as $M_r=6.3\%$ [19].

Table 1 – Elastic and hygrothermal properties of fiber and matrix [1].

Material	E ₁ (GPa)	E ₂ (GPa)	G ₁₂ (GPa)	v	α (10 ⁻⁶ /°F)	β	<i>T</i> _{go} (°F)
Fiber (AS)	214	14	14	0.2	-0.55	0	-
Matrix (HM*)	5.2	5.2	1.93	0.35	40	0.33	420

HM refers to high modulus typical epoxy matrix resin.

Figure 2 depicts the FE mesh, boundary conditions and in-plane loads. A deterministic buckling analysis is then carried out with all random fields taking their mean values as a constant value throughout the plate, with no fluctuations, which in the case of the present study, is obtained by setting all random variables of Eq. 1, in each random field, as zero. The deterministic critical buckling load obtained with Solution 105 of MSC Nastran is $N_{\rm r}^M = 27.83 {\rm N/mm}$.

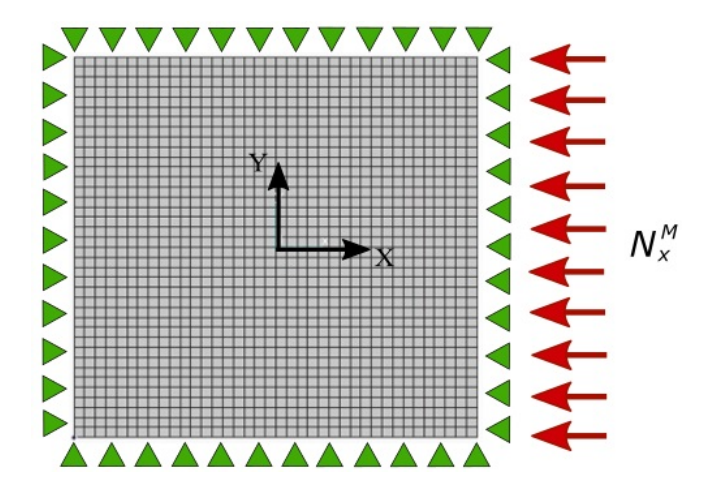


Figure 2 – Finite element model of the composite laminated plate.

3.2 Uncertainty Propagation

Uncertainty propagation is conducted aiming at characterizing the stochastic buckling response of the composite laminate plate considered herein, as described in section 3.1, under the random fields of temperature, fiber-direction angle, ply thickness, and fiber volume fraction.

The non-Gaussian probabilistic distributions assumed for each random field is presented in Table 2, along with the standard deviations adopted. Three different values of coefficient of variation (CV), which is the ratio of the standard deviation to the mean of the random field, are analyzed: 0.01, 0.03, and 0.05. In the case of the spatially varying fiber angle, as the degree of accuracy of manual or automated lamination processes determines such manufacturing uncertainties, independently of the angle value, it was found reasonable to consider the same standard deviation value, in each analysis, simultaneously to all fiber angle random fields, as per Table 2.

Regarding the covariance function assigned to the random fields, the following exponential one is adopted:

$$C(\zeta_1, \zeta_2; \eta_1, \eta_2) = \sigma_N^2 e^{-|\zeta_1 - \zeta_2|/l_{\zeta} - |\eta_1 - \eta_2|/l_{\eta}} , \qquad (28)$$

where l_{ζ} and l_{η} are the correlation lengths (CLs) in the ζ and η directions, respectively. In this work, the same value of CL is assigned simultaneously in ζ and η directions (i.e, $l_{\zeta} = l_{\eta}$).

Table 2 – Probabilistic distributions, mean values and standard deviations assumed for all random fields in the stochastic analysis.

Random Field	Distribution	Mean (μ_N)	Standard Deviation (σ_N)			
			CV=0.01	CV=0.03	CV=0.05	
Temperature (°F)	Log-Normal	120	1.2	3.6	6.0	
Ply thickness (mm)**	Log-Normal	0.2	0.002	0.006	0.010	
Fiber Volume fraction**	Log-Normal	0.6	0.006	0.018	0.030	
Fiber angle (°)**	Uniform	***	0.58 (-1,+1)*	1.73 (-3,+3)*	2.89 (-5,+5)*	

^{*} In parentheses, the bounds of uniform distribution.

Two values of CL are considered in the uncertainty propagation: 0.10 and 1.0. Due to the influence of the value of CL in the discretization of the random field by KLE, an appropriate choice of the number of terms kept in the truncated series expansion is required. The eigenvalues from Eq. 2 are sorted in decreasing order and, based on [22], the number of retained eigensolutions is determined by comparing the sum of the neglected eigenvalues with the sum of retained ones, where the first should be sufficiently small compared to the second; a ratio of 5% is chosen. As a result, for CLs of 0.10 and 1.0, 334 and 61 random variables (ξ_n) are used for random field discretization, respectively. Sampling-based statistics of the critical buckling load are obtained from MCS method combined with the LHS. For each combination of values of CV and CL, 5,000 sample sets of random variables were generated, where, with a total of 91 random fields (as per Table 2), each set is constituted by 30,394 and 5,551 random variables for CLs of 0.10 and 1.0, respectively.

In Figure 3, the spatial distributions of each random field with different CLs are illustrated considering a fixed CV of 0.03, for exemplification, and choosing randomly one sample set and a lamina for which the random field is associated. All portrayed random fields present high spatial frequency of variation when the smaller correlation length is employed, whereas a smoother variation is exhibited when the CL is increased.

In each stochastic analysis of determined combination of CV and CL values, for each sample set generated, a FEM is built and analyzed in the Solution 105 of MSC Nastran to compute the critical buckling load from Eq.27. Histograms of the resulting buckling load samples are plotted on Figure 4, where the characteristics of the probability distributions, namely mean (μ_B) , standard deviation (σ_B) , coefficient of variation (CV_B) , skewness (Skn) and kurtosis (Kts), are also depicted. One should note that negative buckling loads, indicated in red on the histogram in Figure 4 (f), denote samples where only the higrothermal load with no axial load leads the plate to buckling.

It can be noticed from Figure 4 that larger dispersion of buckling loads is observed when standard deviation of the random fields increases, as expected. Also, when the correlation length is increased, higher CV values of responses are observed, which can be explained by a magnification of variations in scenarios of low frequency deviations, where any fluctuations extend over a larger area of the structure.

A linear relationship is also verified in Figure 4 between CV values adopted for random fields and those obtained for buckling responses, while a nonlinear relationship is observed between CL and the coefficient of variation of the critical buckling load. Furthermore, the skewness and kurtosis obtained indicate that response distributions exhibit approximate symmetry (skewness values near zero) and have longer and thicker tails compared to normal distribution (kurtosis values greater than 3.0).

^{**} For each lamina, totaling 30 random fields.

^{***} The mean value of each fiber-direction angle random field is according the lamina angle in the lamination sequence.

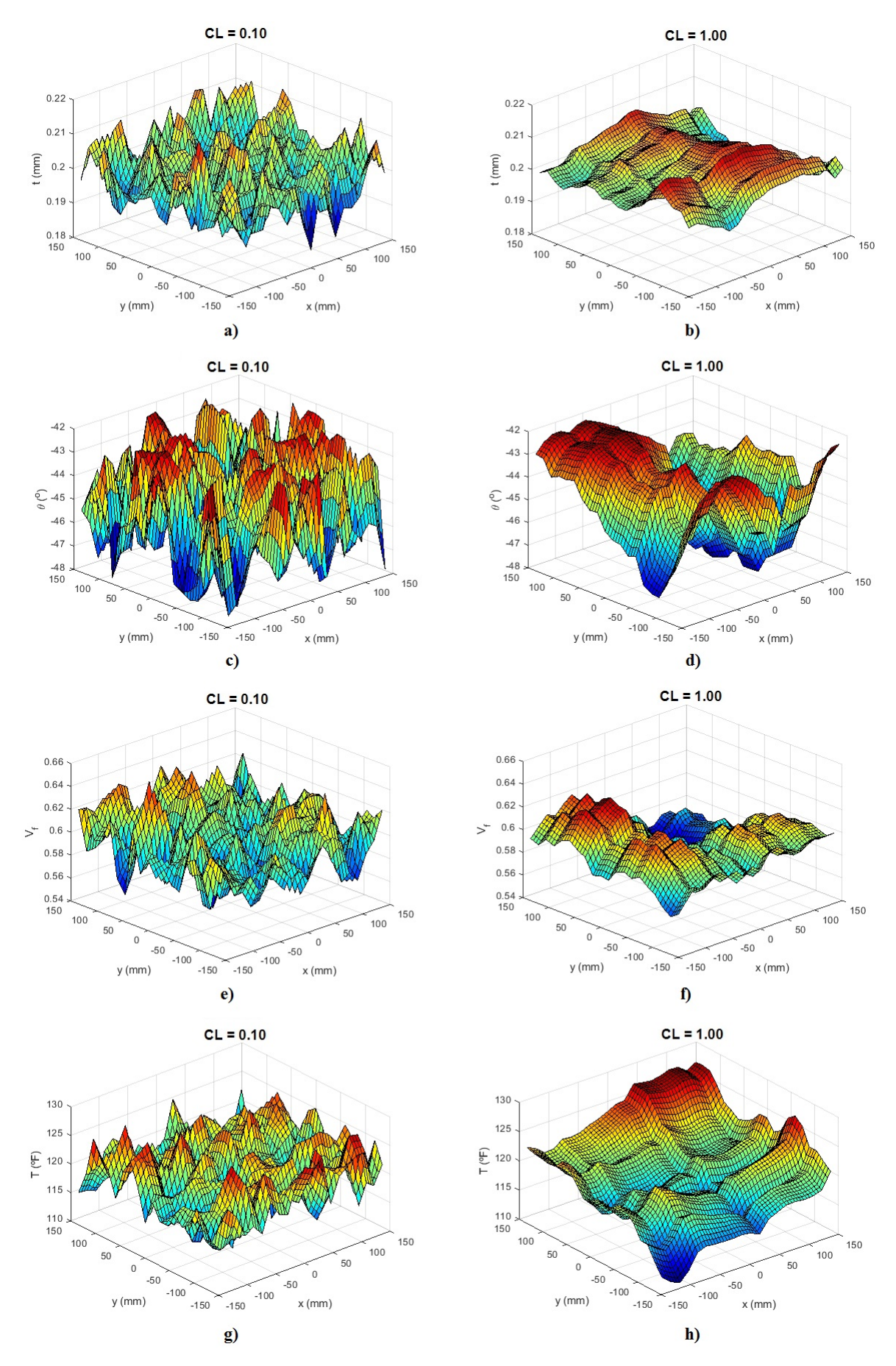


Figure 3 – Samples of random fields: ply thickness (a,b), fiber-direction angle (c,d), fiber volume fraction (e,f), and temperature (g,h) distributions on laminate plate for CLs of 0.10 and 1.00.

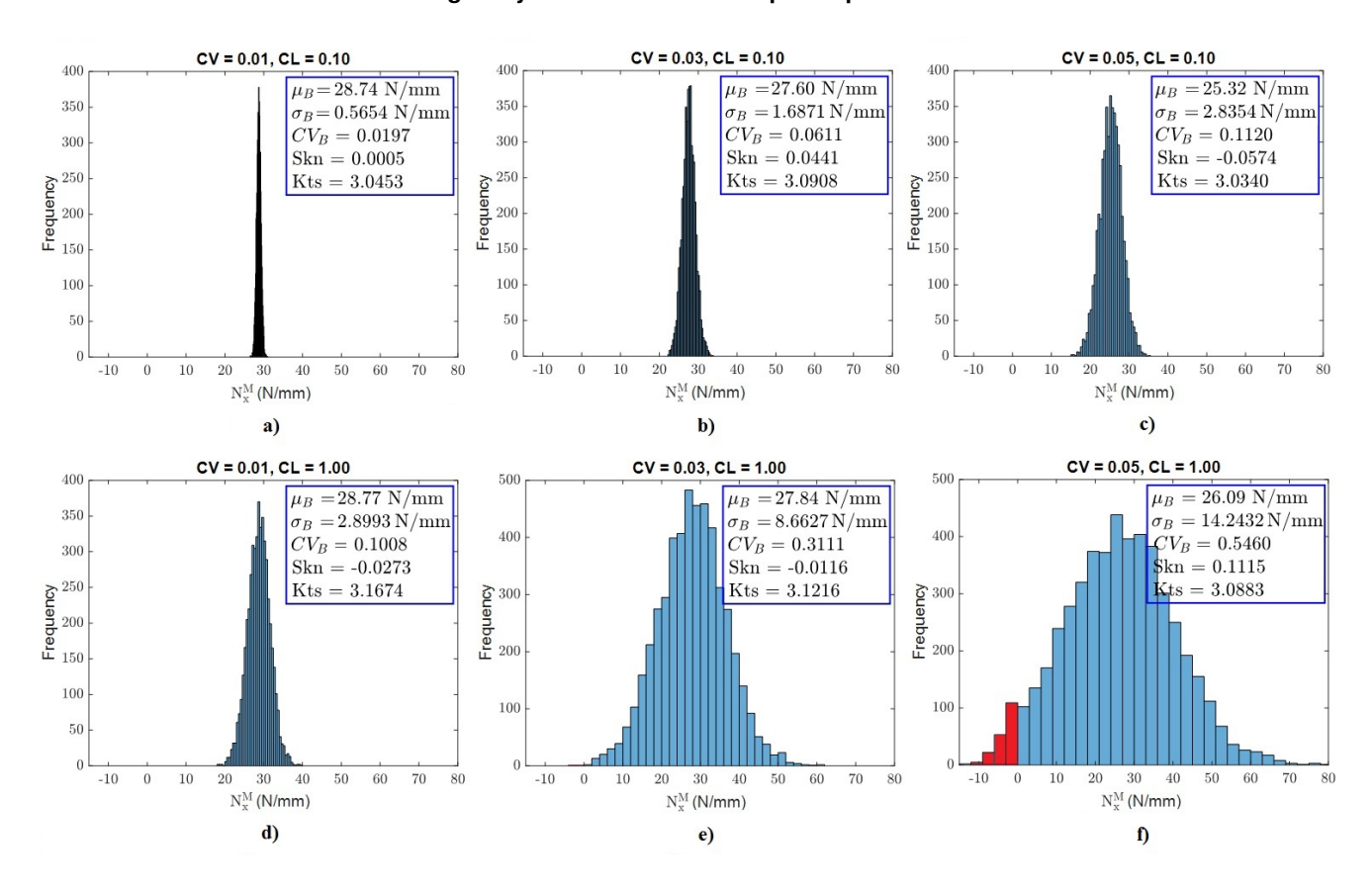


Figure 4 – Results of critical buckling load statistics regarding each stochastic analysis: a) CV=0.01, CL=0.10; b) CV=0.03, CL=0.10; c) CV=0.05, CL=0.10; d) CV=0.01, CL=1.00; e) CV=0.03, CL=1.00; f) CV=0.05, CL=1.00.

4. Conclusions

The stochastic evaluation of buckling response of a laminated composite plate under temperature, fiber-direction angle, ply thickness, and fiber volume fraction random fields was numerically assessed in this work. The discretization of random fields was performed using the Karhunen-Loève Expansion with the methodology KL-ITAM to deal with non-Gaussian distributions. Based on the assumptions of the Classical Lamination Theory, uncertainties in environmental-dependent material properties and in hygrothermally-induced stresses are predicted with the use of micromechanical approach. Added to geometry variabilities, such uncertainties are simultaneously included in a finite element model. Considering different values of standard deviation and correlation length associated to the random fields, uncertainty propagation has been performed using Monte Carlo Simulation combined with Latin Hypercube Sampling. The stochastic critical buckling load demonstrated increasing variation as the standard deviation of the random fields is increased and/or the correlation length assigned to the random fields presents higher value.

Based on the ensemble of results, in a probabilistic framework, this work presented a methodology to incorporate non-Gaussian hygrothermal, geometric and material properties uncertainties in the buckling analysis of composite laminates. Significant dispersion in buckling response enables to justify the importance of incorporating such uncertainties in the analysis and design of aerospace composite structures.

5. Contact Author Email Address

E-mail addresses: henriqueheaas@ita.br (Henrique E. A. A. dos Santos) and rade@ita.br (Domingos A. Rade).

6. Copyright Statement

The authors confirm that they, and/or their company or organization, hold copyright on all of the original material included in this paper. The authors also confirm that they have obtained permission, from the copyright holder of any third party material included in this paper, to publish it as part of their paper. The authors confirm that they give permission, or have obtained permission from the copyright holder of this paper, for the publication and distribution of this paper as part of the ICAS proceedings or as individual off-prints from the proceedings.

7. ACKNOWLEDGEMENTS

The authors acknowledge Embraer S.A. for all the support through the project ATED (Enabled Design by Aeroelastic Tailoring). H.E.A.A. dos Santos acknowledges the Brazilian Ministry of Education (CAPES Foundation) for granting him a PhD scholarship. D.A. Rade acknowledges the support provided by the São Paulo Research Foundation - FAPESP (grants #2018/15894-0 and #2021/11258-5) and the Brazilian Research Council (CNPq) (grants #312068/2020-4 and #407545/2022-0).

References

- [1] Ronald F. Gibson. Principles of Composite Material Mechanics. CRC Press, 3rd edition, 2012.
- [2] X.-Y. Zhou, P.D. Gosling, Z. Ullah, L. Kaczmarczyk, and C.J. Pearce. Stochastic multi-scale finite element based reliability analysis for laminated composite structures. *Applied Mathematical Modelling*, 45:457–473, 2017.
- [3] B.P. Patel, M. Ganapathi, and D.P. Makhecha. Hygrothermal effects on the structural behaviour of thick composite laminates using higher-order theory. *Composite Structures*, 56:25–34, 2002.
- [4] AK Upadhyay, Ramesh Pandey, and KK Shukla. Nonlinear flexural response of laminated composite plates under hygro-thermo-mechanical loading. *Communications in Nonlinear Science and Numerical Simulation*, 15(9):2634–2650, 2010.
- [5] Fei Li and G.J. Nie. Thermo-mechanical buckling analysis of symmetric vat composite laminates with temperature-dependent material properties. *Thin-Walled Structures*, 140:263–271, 2019.
- [6] B. N. Singh and V. K. Verma. Hygrothermal effects on the buckling of laminated composite plates with random geometric and material properties. *Journal of Reinforced Plastics and Composites*, 28:409–427, 2009.
- [7] Narayan Sharma, Mohamed Nishad, Dipak Kumar Maiti, Mohammed Rabius Sunny, and Bhrigu Nath Singh. Uncertainty quantification in buckling strength of variable stiffness laminated composite plate under thermal loading. *Composite Structures*, 275:114486, 2021.
- [8] Rajesh Kumar, H. S. Patil, and A. Lal. Hygrothermoelastic buckling response of laminated composite plates with random system properties: Macromechanical and micromechanical model. *J. Aerosp. Eng.*, 28:04014123, 2015.
- [9] Roger G. Ghanem and Pol D. Spanos. *Stochastic Finite Elements: A Spectral Approach.* Springer-Verlag New York Inc., New York, 1991.
- [10] Wolfgang Betz, Iason Papaioannou, and Daniel Straub. Numerical methods for the discretization of random fields by means of the karhunen–loève expansion. *Computer Methods in Applied Mechanics and Engineering*, 271:109–129, 2014.
- [11] Hwanpyo Kim and Michael D Shields. Modeling strongly non-gaussian non-stationary stochastic processes using the iterative translation approximation method and karhunen–loève expansion. *Computers & Structures*, 161:31–42, 2015.
- [12] S Naskar, T Mukhopadhyay, and S Sriramula. Probabilistic micromechanical spatial variability quantification in laminated composites. *Composites Part B: Engineering*, 151:291–325, 2018.
- [13] T. A. M. Guimarães, H. L. Silva, D. A. Rade, and C. E. S. Cesnik. Aeroelastic stability of conventional and tow-steered composite plates under stochastic fiber volume. *AIAA Journal*, 58(6):2748–2759, 2020.
- [14] Alberto Racionero Sanchez-Majano, Alfonso Pagani, Marco Petrolo, and Chao Zhang. Buckling sensitivity of tow-steered plates subjected to multiscale defects by high-order finite elements and polynomial chaos expansion. *Materials*, 14(11):2706, 2021.
- [15] Hadi Parviz, Mahdi Fakoor, and Fatemeh Hosseini. Probabilistic thermal stability of laminated composite plates with temperature-dependent properties under a stochastic thermal field. *Acta Mechanica*, 233(4):1351–1370, 2022.
- [16] Wolfgang Betz, Iason Papaioannou, and Daniel Straub. Numerical methods for the discretization of random fields by means of the karhunen–loève expansion. *Computer Methods in Applied Mechanics and Engineering*, 271:109–129, 2014.

Stochastic buckling analyses of laminated composite plates under non-Gaussian random fields

- [17] C. C. Chamis and J. H. Sinclair. Durability/life of fiber composites in hygrothermomechanical environments. In *Conf. on Composite Mater.: Testing and Design sponsored by the Am. Soc. for Testing and Mater.*, number E-1065, 1981.
- [18] C. C. Chamis. Simplified composite micromechanics equations for mechanical, thermal, and moisture-related properties. *Engineers' Guide to Composite Materials*, pages 3–8, 1987.
- [19] Alfred C Loos and George S Springer. Moisture absorption of graphite-epoxy composites immersed in liquids and in humid air. *Journal of Composite Materials*, 13(2):131–147, 1979.
- [20] Bhagwan D. Agarwal, Lawrence J. Broutman, and K. Chandrashekhara. *Analysis and performance of fiber composites*. John Wiley & Sons, 3rd edition, 2006.
- [21] MSC Software Corporation. MSC Nastran Linear Static Analysis User's Guide. Newport Beach, CA, 2024
- [22] Ralph C. Smith. *Uncertainty quantification*. SIAM Society for Industrial and Applied Mathematics, Philadelphia, 2013.